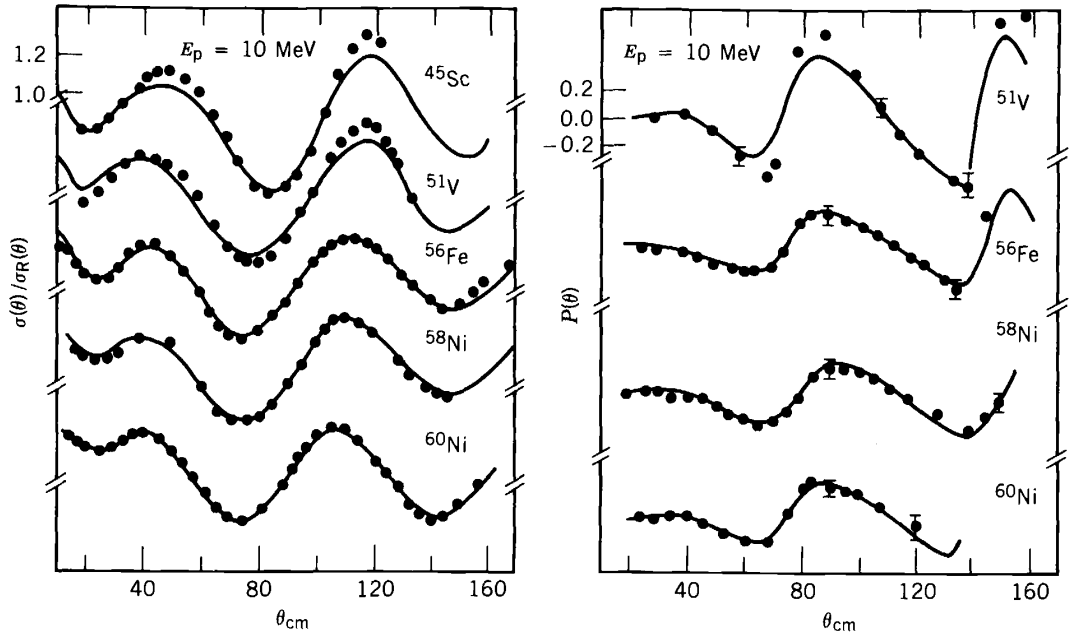

Figure 11.18 Optical-model fits to differential cross sections (at left, shown as a ratio to the Rutherford cross section) and polarizations, for 10-MeV protons scattered elastically from various targets. The solid lines are the fits to the data using the best set of optical-model parameters. From F. D. Becchetti, Jr., and G. W. Greenlees, *Phys. Rev.* **182**, 1190 (1969).

11.10 COMPOUND-NUCLEUS REACTIONS

Suppose an incident particle enters a target nucleus with an impact parameter small compared with the nuclear radius. It then will have a high probability of interacting with one of the nucleons of the target, possibly through a simple scattering. The recoiling struck nucleon and the incident particle (now with less energy) can each make successive collisions with other nucleons, and after several such interactions, the incident energy is shared among many of the nucleons of the combined system of projectile + target. The average increase in energy of any single nucleon is not enough to free it from the nucleus, but as many more-or-less random collisions occur, there is a statistical distribution in energies and a small probability for a single nucleon to gain a large enough share of the energy to escape, much as molecules evaporate from a hot liquid.

Such reactions have a definite intermediate state, after the absorption of the incident particle but before the emission of the outgoing particle (or particles). This intermediate state is called the *compound nucleus*. Symbolically then the reaction a + X → Y + b becomes

$$a + X \rightarrow C^* \rightarrow Y + b$$

where C* indicates the compound nucleus.

As might be assumed from seeing the reaction written in this form, we can consider a reaction that proceeds through the compound nucleus to be a two-step process: the formation and then the subsequent decay of the compound nucleus. A given compound nucleus may decay in a variety of different ways, and essential to the compound-nucleus model of nuclear reactions is the assumption that *the*

relative probability for decay into any specific set of final products is independent of the means of formation of the compound nucleus. The decay probability depends only on the total energy given to the system; in effect, the compound nucleus "forgets" the process of formation and decays governed primarily by statistical rules.

Let's consider a specific example. The compound nucleus $^{64}Zn^*$ can be formed through several reaction processes, including $p + {}^{63}Cu$ and $\alpha + {}^{60}Ni$. It can also decay in a variety of ways, including $^{63}Zn + n$, $^{62}Zn + 2n$, and $^{62}Cu + p + n$. That is

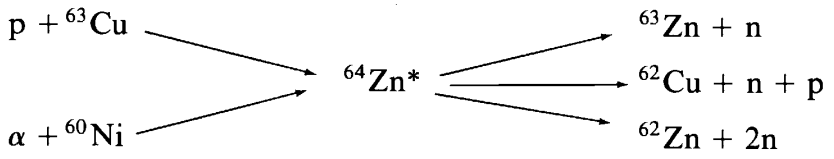

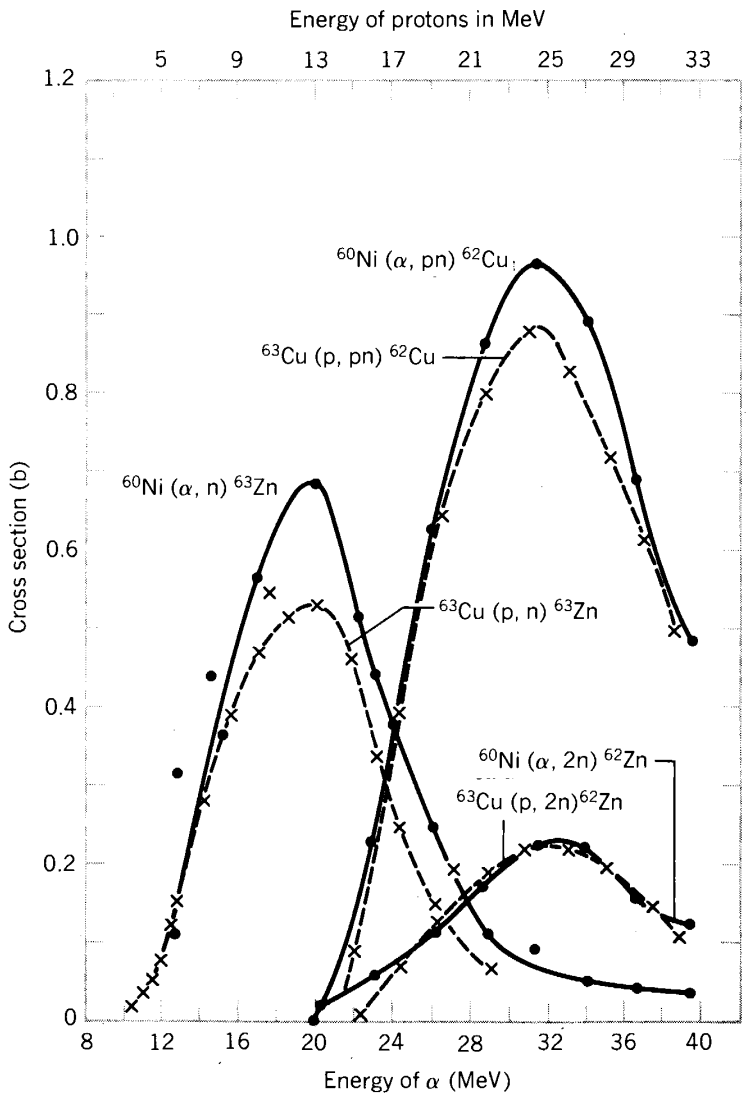

Figure 11.19 Cross sections for different reactions leading to the compound nucleus ^{64}Zn show very similar characteristics, consistent with the basic assumptions of the compound nucleus model. From S. N. Goshal, *Phys. Rev.* **80**, 939 (1950).

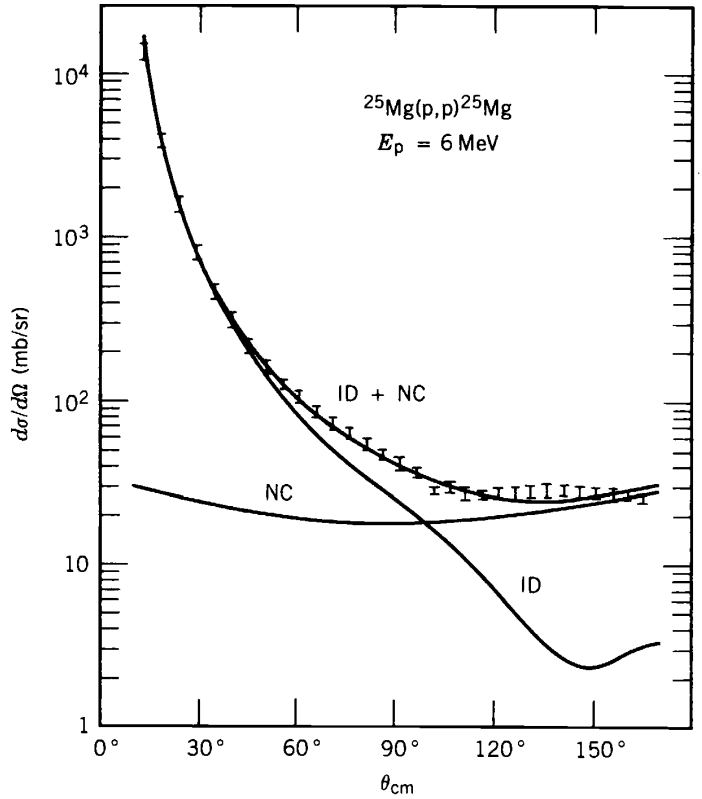

Figure 11.20 The curve marked NC shows the contribution from compound-nucleus formation to the cross section of the reaction ^{25}Mg(p, p)^{25}Mg. The curve marked ID shows the contribution from direct reactions. Note that the direct part has a strong angular dependence, while the compound-nucleus part shows little angular dependence. From A. Gallmann et al., *Nucl. Phys.* **88**, 654 (1966).

If this model were correct, we would expect for example that the relative cross sections for ^{63}Cu(p, n)^{63}Zn and ^{60}Ni(α, n)^{63}Zn would be the same at incident energies that give the same excitation energy to ^{64}Zn*. Figure 11.19 shows the cross sections for the three final states, with the energy scales for the incident protons and α's shifted so that they correspond to a common excitation of the compound nucleus. The agreement between the three pairs of cross sections is remarkably good, showing that indeed, the decay of ^{64}Zn* into any specific final state is nearly independent of how it was originally formed.

The compound-nucleus model works best for low incident energies (10–20 MeV), where the incident projectile has a small chance of escaping from the nucleus with its identity and most of its energy intact. It also works best for medium-weight and heavy nuclei, where the nuclear interior is large enough to absorb the incident energy.

Another characteristic of compound-nucleus reactions is the angular distribution of the products. Because of the random interactions among the nucleons, we expect the outgoing particle to be emitted with a nearly isotropic angular distribution (that is, the same in all directions). This expectation is quite consistent with experiment, as shown in Figure 11.20. In cases in which a heavy ion is the incident particle, large amounts of angular momentum can be transferred to the compound nucleus, and to extract that angular momentum the

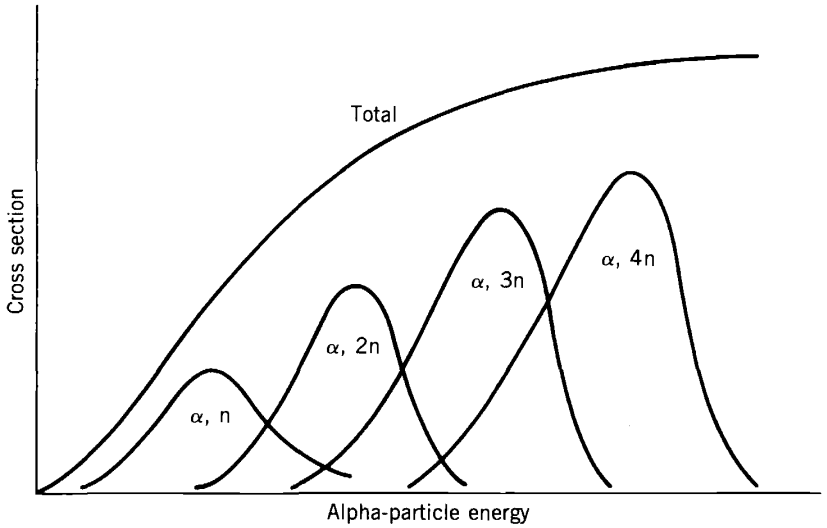

Figure 11.21 At higher incident energies, it is more likely that additional neutrons will "evaporate" from the compound nucleus.

emitted particles tend to be emitted at right angles to the angular momentum, and thus preferentially at 0 and 180°. With light projectiles, this effect is negligible.

The "evaporation" analogy mentioned previously is really quite appropriate. In fact, the more energy we give to the compound nucleus, the more particles are likely to evaporate. For each final state, the cross section has the Gaussian-like shape shown in Figure 11.19. Figure 11.21 shows the cross sections for $(\alpha, x\text{n})$ reactions, where $x = 1, 2, 3, \ldots$. For each reaction, the cross section increases to a maximum and then decreases as the higher energy makes it more likely for an additional neutron to be emitted.

11.11 DIRECT REACTIONS

At the opposite extreme from compound-nucleus reactions are *direct* reactions, in which the incident particle interacts primarily at the surface of the target nucleus; such reactions are also called *peripheral* processes. As the energy of the incident particle is increased, its de Broglie wavelength decreases, until it becomes more likely to interact with a nucleon-sized object than with a nucleus-sized object. A 1-MeV incident nucleon has a de Broglie wavelength of about 4 fm, and thus does not "see" individual nucleons; it is more likely to interact through a compound-nucleus reaction. A 20-MeV nucleon has a de Broglie wavelength of about 1 fm and therefore may be able to participate in direct processes. Direct processes are most likely to involve one nucleon or very few valence nucleons near the surface of the target nucleus.

Of course, it may be possible to have direct and compound-nucleus processes both contribute to a given reaction. How can we distinguish their contributions or decide which may be more important? There are two principal differences that can be observed experimentally: (1) Direct processes occur very rapidly, in a time of the order of 10^{-22} s, while compound-nuclear processes typically take much longer, perhaps 10^{-16} to 10^{-18} s. This additional time is necessary for the

distribution and reconcentration of the incident energy. There are ingenious experimental techniques for distinguishing between these two incredibly short intervals of time. (2) The angular distributions of the outgoing particles in direct reactions tend to be more sharply peaked than in the case of compound-nuclear reactions.

Inelastic scattering could proceed either through a direct process or a compound nucleus, largely depending on the energy of the incident particle. The *deuteron stripping reaction* (d, n), which is an example of a *transfer reaction* in which a single proton is transferred from projectile to target, may also go by either mechanism. Another deuteron stripping reaction (d, p) may be more likely to go by a direct process, for the "evaporation" of protons from the compound nucleus is inhibited by the Coulomb barrier. The (α, n) reaction is less likely to be a direct process, for it would involve a single transfer of three nucleons into valence states of the target, a highly improbable process.

One particularly important application of single-particle transfer reactions, especially (d, p) and (d, n), is the study of low-lying shell-model excited states. Several such states may be populated in a given reaction; we can choose a particular excited state from the energy of the outgoing nucleon. Once we have done so, we would like to determine just which shell-model state it is. For this we need the angular distribution of the emitted particles, which often give the spin and parity of the state that is populated in a particular reaction. Angular distributions therefore are of critical importance in studies of transfer reactions. (*Pickup reactions*, for example (p, d), in which the projectile takes a nucleon from the target, also give information on single-particle states.)

Let's consider in somewhat more detail the angular momentum transfer in a deuteron stripping reaction. In the geometry of Figure 11.22, an incident particle with momentum $\boldsymbol{p}_a$ gives an outgoing particle with momentum $\boldsymbol{p}_b$, while the residual nucleus (target nucleus plus transferred nucleon) must recoil with momentum $\boldsymbol{p} = \boldsymbol{p}_a - \boldsymbol{p}_b$. In a direct process, we may assume that the transferred nucleon instantaneously has the recoil momentum and that it must be placed in an orbit with orbital angular momentum $\ell = Rp$, assuming that the interaction

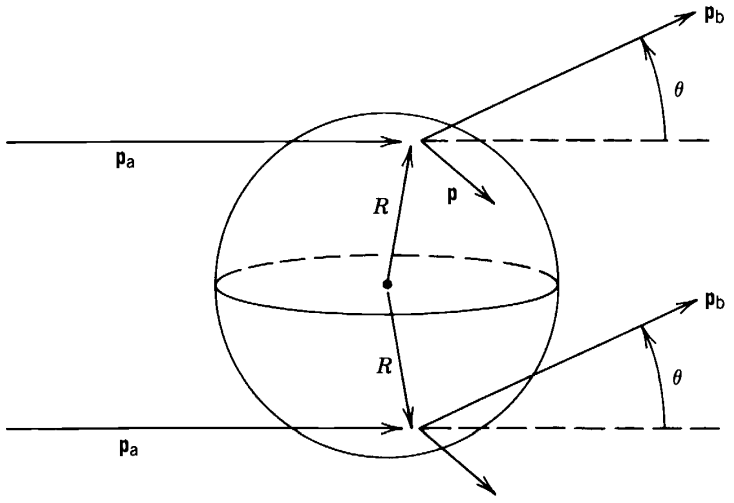

Figure 11.22 Geometry for direct reactions occurring primarily on the nuclear surface.

takes place at the surface of the nucleus. The momentum vectors are related by the law of cosines:

$$p^2 = p_a^2 + p_b^2 - 2p_a p_b \cos\theta$$
$$= (p_a - p_b)^2 + 2p_a p_b(1 - \cos\theta) \qquad (11.57)$$

Given the energies of the incident and outgoing particles, we then have a direct relationship between ℓ and θ—particles emerging at a given angle should correspond to a specific angular momentum of the orbiting particle.

Consider a specific example, the (d, p) reaction on ^{90}Zr leading to single neutron shell-model states in ^{91}Zr. The Q value is about 5 MeV, so an incident deuteron at 5 MeV gives a proton at about 10 MeV, less any excitation in ^{91}Zr. Since at these energies $p_a \simeq p_b \simeq 140$ MeV/c, Equation 11.57 gives

$$\ell = \left[\frac{2c^2 p_a p_b(2\sin^2\theta/2)}{\hbar^2c^2/R^2}\right]^{1/2} \cong 8\sin\frac{\theta}{2}$$

For each angular momentum transfer, we expect to find outgoing protons at the following angles: $\ell = 0$, 0°; $\ell = 1$, 14°; $\ell = 2$, 29°; $\ell = 3$, 44°.

This simple semiclassical estimate will be changed by the intrinsic spins of the particles, which we neglected. There will also be interference between scatterings that occur on opposite sides of the nucleus, as shown in Figure 11.22. These interferences result in maxima and minima in the angular distributions.

Figure 11.23 shows the result of studies of (d, p) reactions on ^{90}Zr. You can see several low-lying states in the proton spectrum, and from their angular distributions we can assign them to specific spins and parities in ^{91}Zr. Notice the appearance of maxima and minima in the angular distribution. The angular momentum transfer, as usual, also gives us the change in parity of the reactions, ℓ = even for no change in parity and ℓ = odd for a change in parity. If we are studying shell-model states in odd-A nuclei by single-particle transfer reactions such as (d, p), we will use an even-Z, even-N nucleus as target, and so the initial spin and parity are 0^+. If the orbital angular momentum transferred is ℓ, then the final nuclear state reached will be $\ell \pm \frac{1}{2}$, allowing for the contribution of the spin of the transferred nucleon. For $\ell = 2$, for instance, we can reach states of $j = \frac{3}{2}$ or $\frac{5}{2}$, both with even parity.

The complete theory of direct reactions is far too detailed for this text, but we can sketch the outline of the calculation as an exercise in applications of the principles of quantum mechanics. The transition amplitude for the system to go from the initial state (X + a) to the final state (Y + b) is governed by the usual quantum mechanical matrix element:

$$M = \int \psi_Y^* \psi_b^* V \psi_X \psi_a \, dv \qquad (11.58)$$

The interaction V must be a very complicated function of many nuclear coordinates. A simplifying assumption is the plane-wave *Born approximation*, in which ψ_a and ψ_b are treated as plane waves. Expanding the resulting exponential $e^{i\mathbf{p}\cdot\mathbf{r}/\hbar}$ using a spherical wave expansion of the form of Equation 11.31 and making the simplifying assumption that the interaction takes place on the nuclear

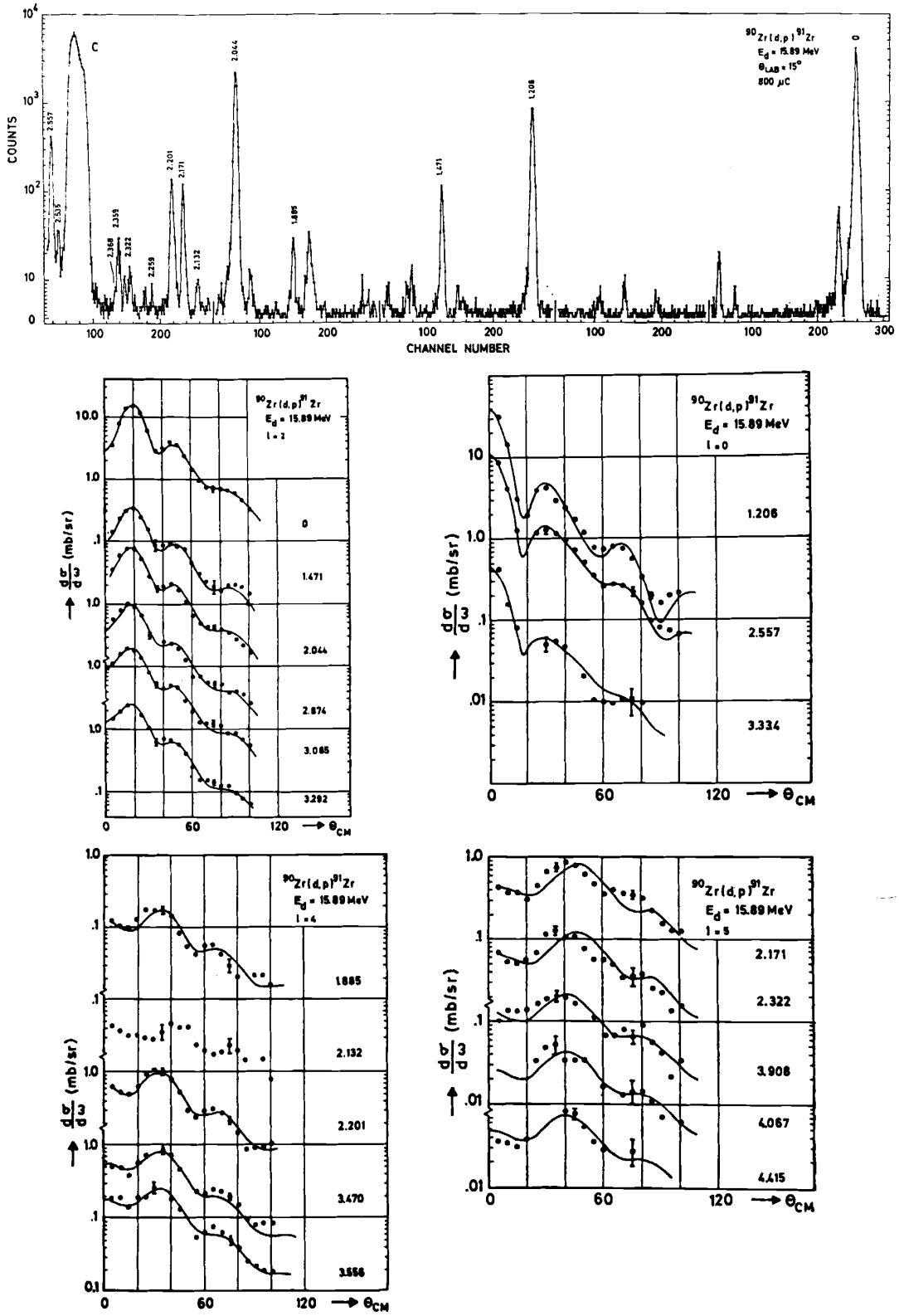

Figure 11.23 (top) Proton spectrum from ^{90}Zr(d, p)^{91}Zr. Peaks are identified with the final states in ^{91}Zr populated. The large peak at the left is from a carbon impurity. (bottom) Angular distributions fitted to determine the ℓ value. Note that the location of the first maximum shifts to larger angles with increasing ℓ, as predicted by Equation 11.57. See Figure 11.24 for the deduced excited states. Data from H. P. Blok et al., *Nucl. Phys. A* **273**, 142 (1976).

surface, so the integral is evaluated only at $r = R$, the matrix element is proportional to $j_\ell(kR)$ where $k = p/\hbar$ contains the explicit angular dependence through Equation 11.57. The cross section then depends on $[j_\ell(kR)]^2$, which gives results of the form of Figure 11.23.

Taking this calculation one step further, we use the optical model to account for the fact that the incoming and outgoing plane waves are changed (or distorted) by the nucleus. This gives the *distorted-wave Born approximation*, or DWBA. We can even put in explicit shell-model wave functions for the final state, and ultimately we find a differential cross section for the reaction. Because there are no "pure" shell-model states, the calculated cross section may describe many different final states. Each will have a differential cross section whose shape can be accurately calculated based on this model, but the amplitude of the cross section for any particular state depends on the fraction of the pure shell-model state included in the wave function for that state. The measured cross section is thus reduced from the calculated shell-model single-particle value by a number

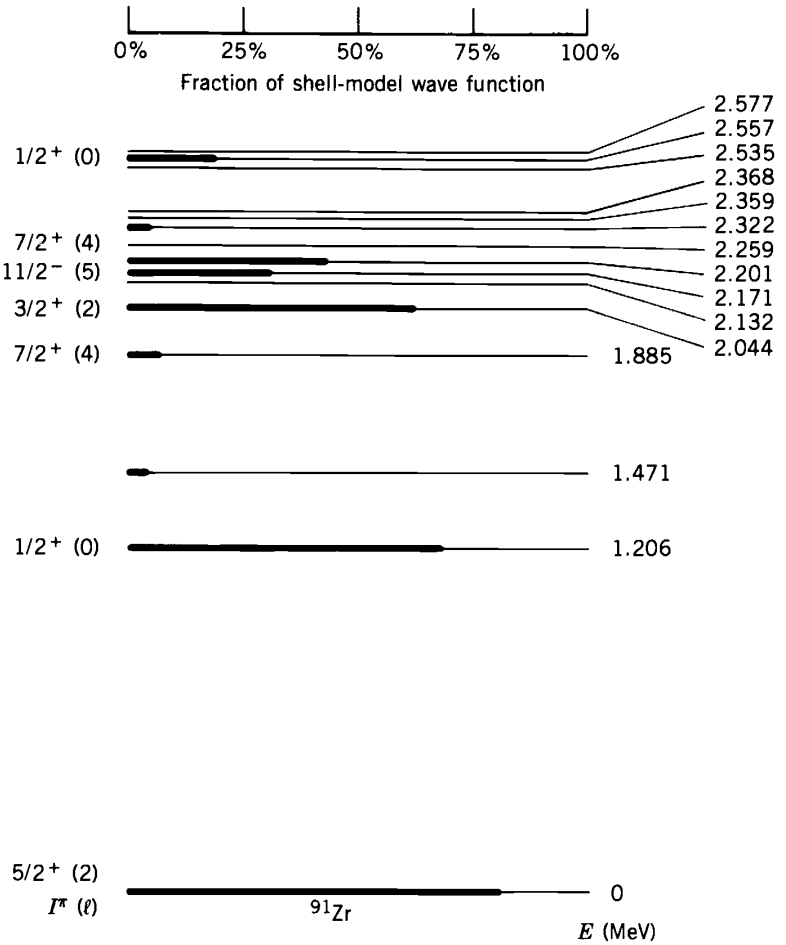

Figure 11.24 Deduced level scheme for ^{91}Zr. Each ℓ value (except zero) deduced from the angular distributions of Figure 11.23 leads to a definite parity assignment but to two possible I values, $\ell \pm \frac{1}{2}$. Which one is correct must be determined from other experiments. The fraction of the single-particle strengths represented by each level is indicated by the length of the shading; thus the ground state is nearly pure $d_{5/2}$ shell-model state.

between 0 and 1 called the *spectroscopic factor* S:

$$\left(\frac{d\sigma}{d\Omega}\right)_{\text{meas}} = S\left(\frac{d\sigma}{d\Omega}\right)_{\text{calc}} \tag{11.59}$$

A pure shell-model state would have $S = 1$. In practice we often find the shell-model wave function to be distributed over many states. Figure 11.24 shows examples of the spectroscopic factors measured for ^{91}Zr.

11.12 RESONANCE REACTIONS

The compound-nucleus model of nuclear reactions treats the unbound nuclear states as if they formed a structureless continuum. That is, there may be discrete nuclear states, but there are so many of them and they are so close together that they form a continuous spectrum. Each of these supposed discrete states is unstable against decay and therefore has a certain *width*; when the states are so numerous that their spacing is much less than the widths of the individual states, the compound-nucleus continuum results.

The bound states studied by direct reactions are at the opposite end of the scale. Because they are stable against particle emission, their mean lives are much longer (for example, characteristic of γ decay) and their corresponding widths are much smaller. A state with a lifetime of 1 ps, for instance, has a width of about 10^{-3} eV, far smaller than the typical spacing of bound states. We are therefore justified in treating these as discrete states with definite wavefunctions.

Between these two extremes is the *resonance* region—discrete levels in the compound-nucleus region. These levels have a high probability of formation (large cross sections), and their widths are very small because at low incident energy, where these resonances are most likely to occur, the quasibound state that is formed usually has only two modes of decay available to it—re-ejecting the incident particle, as in elastic or inelastic scattering, or γ emission.

To obtain a qualitative understanding of the formation of resonances, we represent the nuclear potential seen by the captured particle as a square well. The oscillatory wave functions inside and outside the well must be matched smoothly, as we did in Figure 4.7*a* for nucleon-nucleon scattering. Figure 11.25 shows several examples of how this might occur. Depending on the phase of the wave function inside the nucleus, the smooth matching can result in substantial variations between the relative amplitudes of the wave functions inside and outside the nucleus. In case (*a*), the incident particle has relatively little probability to penetrate the nucleus and form a quasibound state; in case (*c*), there is a very high probability to penetrate. As we vary the energy of the incident particle, we vary the relative phase of the inner and outer wave functions; the location of the matching point *and* the relative amplitudes vary accordingly. Only for certain incident energies do we achieve the conditions shown in part (*c*) of Figure 11.25. These are the energies of the *resonances* in the cross section.

In a single, isolated resonance of energy E_R and width Γ, the energy profile of the cross section in the vicinity of the resonance will have the character of the energy distribution of any decaying state of lifetime $\tau = \hbar/\Gamma$; see, for example, Equation 6.20 or Figure 6.3. The resonance will occur where the total cross

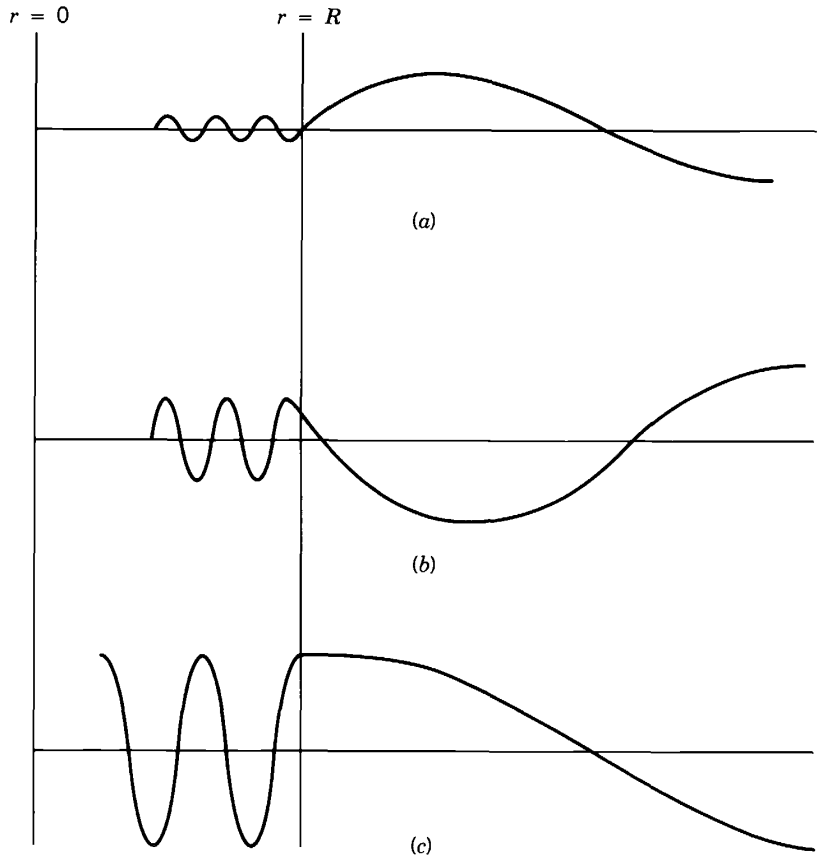

Figure 11.25 (*a*) Far from resonance, the exterior and interior wave functions match badly, and little penetration of the nucleus occurs. (*b*) As the match improves, there is a higher probability to penetrate. (*c*) At resonance the amplitudes match exactly, the incident particle penetrates easily, and the cross section rises to a maximum.

section has a maximum; from Equation 11.48, assuming only one partial wave ℓ is important for the resonant state, there will be a scattering resonance where $\eta_\ell = -1$, corresponding to a phase shift $\delta_\ell = \pi/2$.

The shape of the resonance can be obtained by expanding the phase shift about the value $\delta_\ell = \pi/2$. Better convergence of the Taylor series expansion is obtained if we expand the cotangent of δ_ℓ:

$$\cot \delta_\ell(E) = \cot \delta_\ell(E_R) + (E - E_R)\left(\frac{\partial \cot \delta_\ell}{\partial E}\right)_{E=E_R} + \tfrac{1}{2}(E - E_R)^2\left(\frac{\partial^2 \cot \delta_\ell}{\partial E^2}\right)_{E=E_R} + \cdots \tag{11.60}$$

in which

$$\left(\frac{\partial \cot \delta_\ell}{\partial E}\right)_{E=E_R} = -\left(\frac{\partial \delta_\ell}{\partial E}\right)_{E=E_R} \tag{11.61}$$

Defining the width Γ as

$$\Gamma = 2\left(\frac{\partial \delta_\ell}{\partial E}\right)^{-1}_{E=E_R} \tag{11.62}$$

then it can be shown that the second-order term vanishes, and thus (neglecting higher-order terms)

$$\cot \delta_\ell = -\frac{(E - E_R)}{\Gamma/2} \tag{11.63}$$

Because Γ is the full width of the resonance, the cross section should fall to half of the central value at $E - E_R = \pm\Gamma/2$. From Equation 11.63, this occurs when $\cot \delta_\ell = \pm 1$, or $\delta_\ell = \pi/4, 3\pi/4$ (compared with $\delta_\ell = \pi/2$ at the center of the resonance). The cross section depends on $\sin^2 \delta_\ell$, which does indeed fall to half the central value at $\delta_\ell = \pi/4$ and $3\pi/4$. The width defined by Equation 11.62 is thus entirely consistent with the width shown in Figure 6.3.

From Equation 11.63, we find

$$\sin \delta_\ell = \frac{\Gamma/2}{\left[(E - E_R)^2 + \Gamma^2/4\right]^{1/2}} \tag{11.64}$$

and the scattering cross section becomes, using Equation 11.45

$$\sigma_{sc} = \frac{\pi}{k^2}(2\ell + 1)\frac{\Gamma^2}{(E - E_R)^2 + \Gamma^2/4} \tag{11.65}$$

This result can be generalized in two ways. In the first place, we can account for the effect of reacting particles with spin. If s_a and s_X are the spins of the incident and target particles, and if I is the total angular momentum of the resonance,

$$\boldsymbol{I} = \boldsymbol{s}_a + \boldsymbol{s}_X + \boldsymbol{\ell} \tag{11.66}$$

then the factor $(2\ell + 1)$ in Equation 11.65 should be replaced by the more general statistical factor

$$g = \frac{2I + 1}{(2s_a + 1)(2s_X + 1)} \tag{11.67}$$

Note that g reduces to $(2\ell + 1)$ for spinless particles.

The second change we must make is to allow for partial entrance and exit widths. If the resonance has many ways to decay, then the total width Γ is the sum of all the partial widths Γ_i

$$\Gamma = \sum_i \Gamma_i \tag{11.68}$$

The Γ^2 factor in the denominator of Equation 11.65 is related to the decay width of the resonant state and therefore to its lifetime: $\Gamma = \hbar/\tau$. The observation of only a single entrance or exit channel does not affect this factor, for the resonance always decays with the same lifetime τ. In the analogous situation in

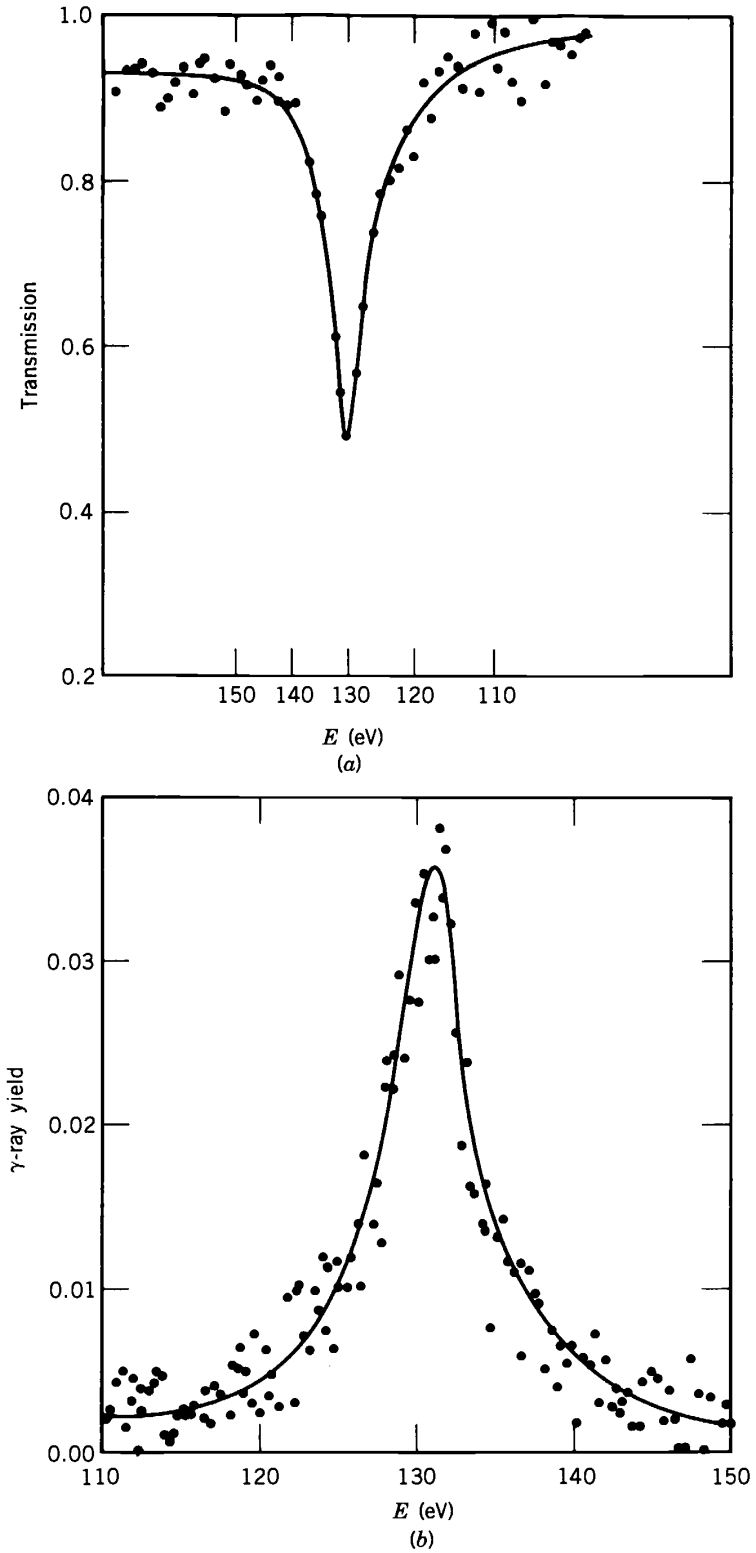

Figure 11.26 130-eV neutron resonance in scattering from ^{59}Co. Part (*a*) shows the intensity of neutrons transmitted through a target of ^{59}Co; at the resonance there is the highest probability for a reaction and the intensity of the transmitted beam drops to a minimum. In (*b*), the γ-ray yield is shown for neutron radiative capture by ^{59}Co. Here the yield of γ rays is maximum where the reaction has the largest probability. From J. E. Lynn, *The Theory of Neutron Resonance Reactions* (Oxford: Clarendon, 1968).

radioactive decay, the activity decays with time according to the total decay constant, even though we might observe only a single branch with a very different partial decay constant. The Γ^2 factor in the numerator, on the other hand, is directly related to the formation of the resonance and to its probability to decay into a particular exit channel. In the case of elastic scattering, for which Equation 11.65 was derived, the entrance and exit channels are identical. That is, for the reaction a + X → a + X, we should use the partial widths Γ_{aX} of the entrance and exit channels:

$$\sigma = \frac{\pi}{k^2} g \frac{(\Gamma_{aX})^2}{(E - E_R)^2 + \Gamma^2/4} \tag{11.69}$$

Similarly, for the reaction a + X → b + Y, a different exit width must be used:

$$\sigma = \frac{\pi}{k^2} g \frac{\Gamma_{aX}\Gamma_{bY}}{(E - E_R)^2 + \Gamma^2/4} \tag{11.70}$$

Equations 11.69 and 11.70 are examples of the *Breit-Wigner formula* for the shape of a single, isolated resonance. Figure 11.26 shows such a resonance with the Breit-Wigner shape. The cross section for resonant absorption of γ radiation has a similar shape, as given by Equations 10.29 and 10.30.

Many elastic scattering resonances have shapes slightly different from that suggested by the Breit-Wigner formula. This originates with another contribution to the reaction amplitude from direct scattering of the incident particle by the nuclear potential, without forming the resonant state. This alternative process is called *potential scattering* or *shape-elastic scattering*. Potential scattering and

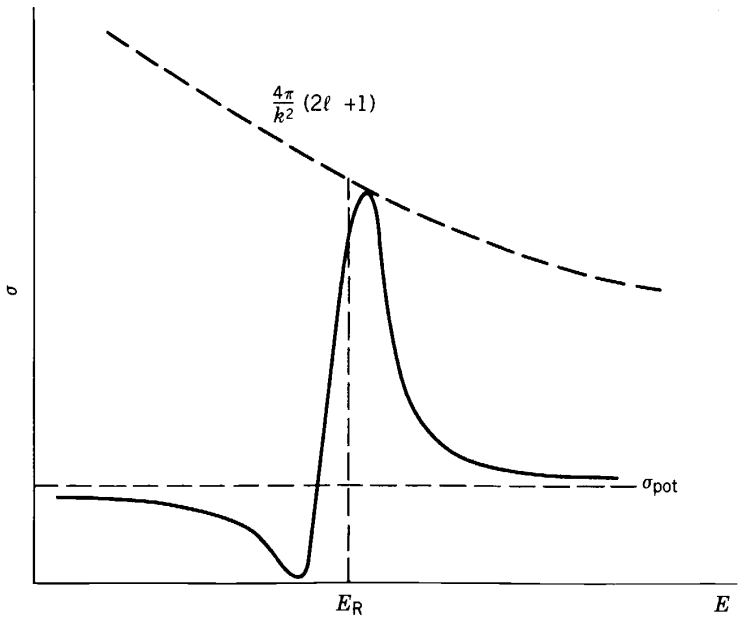

Figure 11.27 Interference between resonance and potential scattering produces resonances with this characteristic shape.

resonant scattering both contribute to the elastic scattering amplitude, and interference between the two processes causes variation in the cross section. Interference can cause the combined cross section to be smaller than it would be for either process alone. It is therefore not correct simply to add the cross sections for the two processes. We can account for the two processes by writing

$$\eta_\ell = e^{2i(\delta_{\ell R}+\delta_{\ell P})} \tag{11.71}$$

where $\delta_{\ell R}$ is the resonant phase shift, as in Equations 11.63 or 11.64, and $\delta_{\ell P}$ is an additional contribution to the phase shift from potential scattering. From

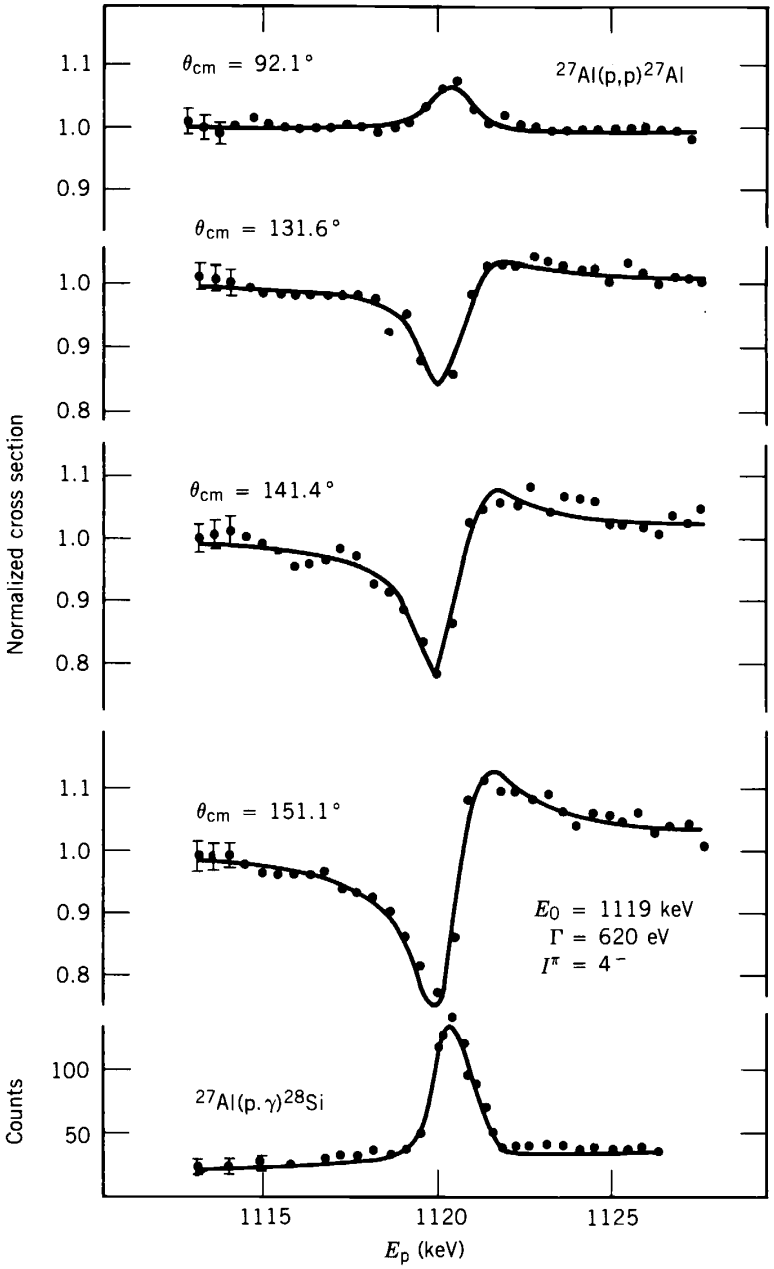

Figure 11.28 Resonances in the reaction ^{27}Al(p, p)^{27}Al. The resonances occur in the nucleus ^{28}Si. Note that the (p, γ) yield shows a resonance at the same energy. From A. Tveter, *Nucl. Phys. A* **185**, 433 (1972).

Equation 11.44 we find the cross section

$$\sigma_{sc} = \frac{\pi}{k^2}(2\ell + 1)\left| e^{-2i\delta_{\ell P}} - 1 + \frac{i\Gamma}{(E - E_R) + i\Gamma/2} \right|^2 \tag{11.72}$$

Far from the resonance, $(E - E_R) \gg \Gamma/2$ and the potential scattering term dominates:

$$\sigma \cong \sigma_{pot} = \frac{4\pi}{k^2}(2\ell + 1)\sin^2 \delta_{\ell P} \tag{11.73}$$

At $E = E_R$, the resonant term dominates and

$$\sigma \cong \sigma_{res} = \frac{4\pi}{k^2}(2\ell + 1) \tag{11.74}$$

Near the resonance there is interference between the two terms, which produces the characteristic shape shown in Figure 11.27. According to this model, we

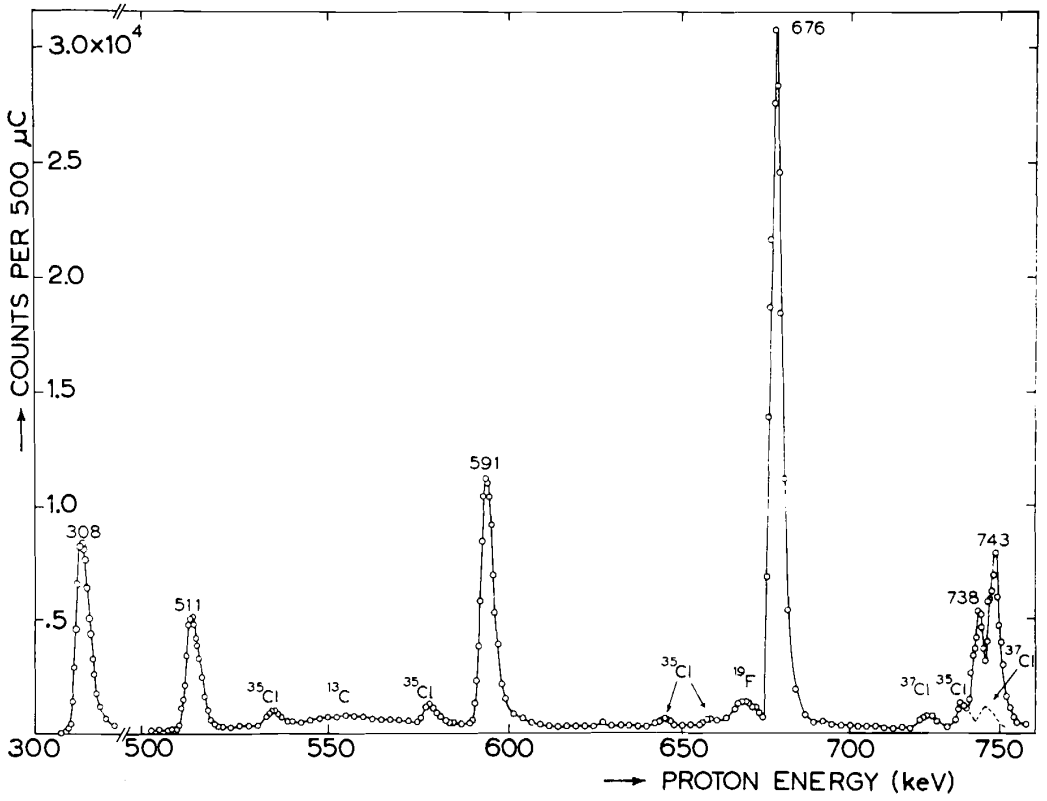

Figure 11.29 Resonances observed in the radiative proton capture by ^{23}Na. In this case, the total yield of γ rays in the energy range 3 – 13 MeV was measured as a function of the incident proton energy. The Cl peaks appear because the target used was NaCl. From P. W. M. Glaudemans and P. M. Endt, *Nucl. Phys.* **30**, 30 (1962).

expect an interference "dip" on the low-E side of the resonance. The resonance height should decrease roughly as k^{-2} (that is, as E^{-1}) with increasing incident energy, and the nonresonant "background" from potential scattering should remain roughly constant. Figure 11.28 shows scattering cross sections with the resonant structure clearly visible. The expectations of the resonance model are clearly fulfilled.

Radiative capture reactions also show a resonant structure. Figure 11.29 shows examples of (p, γ) reactions. Note that this is not a γ spectrum in the conventional sense—the horizontal axis shows the incident proton energy, not the emitted γ energy.

Resonances observed in neutron scattering are discussed in more detail in Chapter 12.

11.13 HEAVY-ION REACTIONS

From the point of view of nuclear reactions, a heavy ion is defined to be any projectile with $A > 4$. Accelerators devoted to the study of heavy-ion reactions can produce beams of ions up to ^{238}U, at typical energies of the order of 1–10 MeV per nucleon, although much higher energies are also possible.

The variety of processes than can occur in heavy-ion reactions is indicated schematically in Figure 11.30. At large impact parameters, Coulomb effects dominate, and Rutherford scattering or Coulomb excitation may occur. When the nuclear densities of the target and projectile just begin to overlap, nuclear reactions can occur, and at small overlap ordinary elastic or inelastic scattering and few-nucleon transfer through direct reactions may occur, as discussed previously in this chapter.

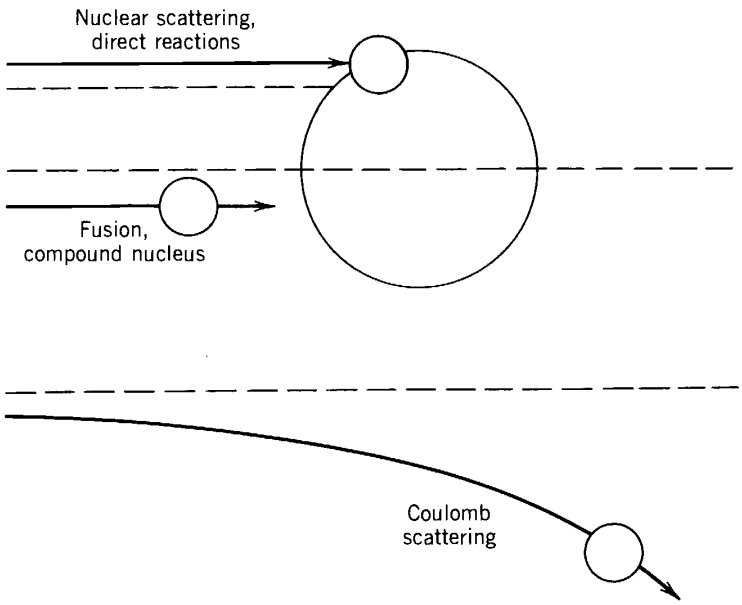

Figure 11.30 Processes in heavy-ion scattering depend on the impact parameter, when energies are large enough to penetrate the Coulomb barrier.